



Computer simulations for the extended Hubbard model utilizing Nonextensive Statistical Mechanics

F. A. R. Navarro* y J. F. V. Flores†

Facultad de Ciencias Físicas, Universidad Nacional Mayor de San Marcos, Lima, Perú

Recibido 25 noviembre 2011 - Aceptado 26 diciembre 2011

We study a system formed by M dimers through half-filled two-site Hubbard model, with two electrons. Our approach use the third version of Nonextensive Statistical Mechanics as tool for calculating thermodynamic and magnetic parameters such as entropy, internal energy, magnetization and specific heat. In the computer simulations, we vary the q entropic index values between 1 and 2, such that, $q = 1.0, 1.4, 1.7$ and 2.0 . These values are interesting to study small magnetic systems. We find the critical temperature regions in simulations with the simple Hubbard model, *i.e.* without the intersite interaction. For other side, adding this additional term, we notice an enlargement and shifting of the thermodynamic parameters comparing with the obtained from simple Hubbard model; even more, we found in some cases the absence of the critical temperature regions.

Keywords: Extended Hubbard, Quantum Statistical Mechanics for nonextensive systems, thermal properties of small particles..

Simulaciones computacionales para el modelo de Hubbard extendido usando la mecánica estadística no extensiva

Estudiamos un sistema formado por M dímeros a través del modelo de Hubbard de dos sitios semillenos, es decir, con dos electrones. Para nuestro enfoque usamos la tercera versión de la mecánica estadística no extensiva como herramienta para calcular los parámetros termodinámicos y magnéticos tales como la entropía, la energía interna, la magnetización y el calor específico. En las simulaciones, variamos los valores del índice entropico q entre 1 y 2, de modo que $q = 1.0, 1.4, 1.7$ y 2.0 . Estos valores son interesantes para el estudio de sistemas magnéticos pequeños. Encontramos regiones de temperatura crítica usando el modelo simple de Hubbard, es decir, sin interacción entre los sitios. por otro lado, añadiendo el término de interacción, encontramos un alargamiento y un corrimiento de los parámetros termodinámicos comparado a los obtenidos mediante el modelo simple. Más aún, encontramos algunos casos en que las regiones de temperatura crítica desaparecen.

Palabras claves: Hubbard extendido, mecánica estadística cuántica para sistema no extensivos, propiedades térmicas de pequeñas partículas..

From all the theories known as the Generalized Statistics, the Nonextensive Statistical Mechanics is widely studied, it is also known as the Tsallis statistics, in tribute to its developer, the Brazilian-Greek born Constantino Tsallis. This statistical theory would be able to generalize the Boltzmann-Gibbs-Shannon statistics.

The great motivation of the present work are the interesting results from recent investigation [1] about magnetic properties of small system with the simple Hubbard model [2–4]. These researches used the Nonextensive Statistical Mechanics to do computer simu-

lations with the Newton-Raphson method.

In this paper, we employ the third version of Tsallis statistics, which was proposed in 1998 [5–7]. We study the extended Hubbard model and found another way of calculating the probabilities, as we explain it below. We discuss the half-filled two-site Hubbard model [8] and the third version of the Nonextensive Statistical Mechanics. Next, we calculate the energy eigenvalues for the Hamiltonian matrix, and also explain how to find the energy eigenvectors. The eigenvalues was used in the thermal average formulas inside the Nonextensive

*farnape@gmail.com

†jventof@unmsm.edu.pe

Statistical Mechanics.

We show the results obtained by the MathLab 7.0 programming language. We calculate the entropy per dimer, internal energy and specific heat per dimer. Finally, we present the conclusions.

Half-filled two-site Hubbard model

The Hubbard model was proposed in the 60's by the British physicist John Hubbard [2]. This model is paradigmatic inside the solid state physics; it is a simple model than take into account particles in interaction in a crystal lattice.

Through this model, complex phenomena have been explained, namely, metal-insulating transition, ferromagnetic and antiferromagnetic phases and even the superconductivity. Despite of simplicity, only a few exact solutions for certain cases are known, and a review can be seen in the literature [2,4]. We analyze a system with M dimers and $N = 2M$ particles.

The simple Hubbard Hamiltonian has three terms. First, a kinetic term that allows the electrons jumping between neighbor sites of a crystal lattice; second, a potential energy term that reckons the on-site Coulombian interaction; and third, a term that take into account the Zeeman effect,

$$\hat{H}_H = -t \sum_{\sigma} \left(c_{1,\sigma}^{\dagger} c_{2,\sigma} + c_{2,\sigma}^{\dagger} c_{1,\sigma} \right) + U \sum_j n_{j,\uparrow} n_{j,\downarrow} - h \sum_j (n_{j,\uparrow} - n_{j,\downarrow}), \quad (1)$$

where σ stand for spines that may be up, (\uparrow) or down, (\downarrow), the indexes j designate number sites of respective dimer, 1 and 2; t is the hopping integral for the kinetic energy term. Also, inside the second quantization framework, $c_{1,\sigma}^{\dagger}$ is the creation operator of a particle in the site 1 with spin, σ ; $c_{2,\sigma}$ is the annihilation operator of a particle with spin σ in the site 2. For the on-site interaction term, U is the potential energy, where $n_{1,\uparrow}$ is the particle number operator in the site 1 with spin \uparrow ; and $n_{1,\downarrow}$ is the particle number operator in the site 1 with spin \downarrow ; the same are replicated for site 2.

Taking into account the extended Hubbard model [8], we add another energy term, the intersite Coulombian interaction

$$\hat{H}_i = J_1 \sum_{\sigma} n_{1,\sigma} n_{2,\sigma} + J_2 \sum_{\sigma} n_{1,\sigma} n_{2,-\sigma}, \quad (2)$$

where J_1 and J_2 are the interactions between next neighbor sites 1 and 2, inside each dimer; they are Coulombian repulsions modified by polaron effects. Consequently, we arrange the total Hamiltonian operator of the dimer as

$$\hat{H}_d = \hat{H}_H + \hat{H}_i. \quad (3)$$

Calculation of energy eigenvalues in the half-filled two-site Hubbard model

In this subsection, our goal is to find the energy eigenvalues, so we must make up the Hamiltonian matrix. Even though we can utilize any arbitrary vector basis, we manipulate the following basis of six vectors

$$\begin{aligned} |\Phi_1\rangle &= |\uparrow\downarrow, 0\rangle, & |\Phi_2\rangle &= |\uparrow, \uparrow\rangle, \\ |\Phi_3\rangle &= |\uparrow, \downarrow\rangle, & |\Phi_4\rangle &= |\downarrow, \uparrow\rangle, \\ |\Phi_5\rangle &= |\downarrow, \downarrow\rangle, & |\Phi_6\rangle &= |0, \uparrow\downarrow\rangle; \end{aligned} \quad (4)$$

the commas separate spins in different sites; if we take the vector basis in a different order, then we get another Hamiltonian matrix, but the eigenvalues will be the same, for instance see [9]. Next, the matrix elements of \hat{H}_d are given by

$$[H_d]_{m,n} = \langle \Phi_m | \hat{H}_d | \Phi_n \rangle, \quad (5)$$

in order to obtain the 36 matrix elements, we apply \hat{H}_d on the base kets, and we get

$$\begin{aligned} \hat{H}_d |\Phi_1\rangle &= -t(|\Phi_4\rangle + |\Phi_3\rangle) + U|\Phi_1\rangle, \\ \hat{H}_d |\Phi_2\rangle &= (J_1 - 2h)|\Phi_2\rangle, \\ \hat{H}_d |\Phi_3\rangle &= -t(|\Phi_1\rangle + |\Phi_6\rangle) + J_2|\Phi_3\rangle, \\ \hat{H}_d |\Phi_4\rangle &= -t(|\Phi_1\rangle + |\Phi_6\rangle) + J_2|\Phi_4\rangle, \\ \hat{H}_d |\Phi_5\rangle &= (J_1 + 2h)|\Phi_5\rangle, \\ \hat{H}_d |\Phi_6\rangle &= -t(|\Phi_3\rangle + |\Phi_4\rangle). \end{aligned} \quad (6)$$

Now, on the left side from these expressions, we apply with the respective bras and we get the following 6×6 Hermitian matrix given by

$$H_d \doteq \begin{pmatrix} U & 0 & -t & -t & 0 & 0 \\ 0 & J_1 - 2h & 0 & 0 & 0 & 0 \\ -t & 0 & J_2 & 0 & 0 & -t \\ -t & 0 & 0 & J_2 & 0 & -t \\ 0 & 0 & 0 & 0 & J_1 + 2h & 0 \\ 0 & 0 & -t & -t & 0 & U \end{pmatrix}, \quad (7)$$

where the symbol \doteq means *represented by*. So, we must diagonalize this matrix to find the eigenvalues, but it is equivalent to the condition $\det[H_d - \lambda I] = 0$ where I is the 6×6 identity matrix. We will apply the properties of determinant for converting it in an upper triangular matrix determinant. The calculation provides the following expression $A = \det[H_d - \lambda I]$, as

$$A = 0 = \begin{vmatrix} U - \lambda & 0 & -t & 0 & 0 & 0 \\ 0 & J_1 - 2h - \lambda & 0 & 0 & 0 & 0 \\ 0 & 0 & J_2 - \lambda & \lambda - J_2 & 0 & 0 \\ 0 & 0 & 0 & X & 0 & -t(U - \lambda)(J_2 - \lambda) \\ 0 & 0 & 0 & 0 & J_1 + 2h - \lambda & 0 \\ 0 & 0 & 0 & 0 & 0 & (U - \lambda)(J_2 - \lambda) \end{vmatrix}; \quad (8)$$

in order to reduce the size of the last equation, we have introduced the symbol X that denotes

$$X = (U - \lambda) \left[(U - \lambda)(J_2 - \lambda)^2 - 2(J_2 - \lambda)t^2 \right] - 2t^2(U - \lambda)(J_2 - \lambda), \quad (9)$$

by know that zero is the product of the diagonal elements, straightaway, we deduce that U , J_2 , $J_1 - 2h$, and $J_1 + 2h$ are four eigenvalues. Obviously, the two remain eigenvalues will come to light from $X = 0$. Simplifying, we get that

$$(U - \lambda)(J_2 - \lambda) - 4t^2 = 0, \quad (10)$$

and solving this 2th-degree equation for λ , we obtain the two other two eigenvalues $C + \frac{U+J_2}{2}$ and $-C + \frac{U+J_2}{2}$. In these expressions we have set another parameter once more,

$$C = \sqrt{\left(\frac{U - J_2}{2}\right)^2 + 4t^2}. \quad (11)$$

Finally, we can establish the six energy eigenvalues as

$$\begin{aligned} \varepsilon_1 &= J_2, \\ \varepsilon_2 &= U, \\ \varepsilon_3 &= C + \frac{U + J_2}{2}, \\ \varepsilon_4 &= -C + \frac{U + J_2}{2}, \\ \varepsilon_5 &= J_1 - 2h, \\ \varepsilon_6 &= J_1 + 2h. \end{aligned} \quad (12)$$

Therefore, we can represent the hamiltonian matrix in the eigenvector basis, even as we don't know it, like to

$$H_d \doteq \begin{pmatrix} \varepsilon_1 & 0 & 0 & 0 & 0 & 0 \\ 0 & \varepsilon_2 & 0 & 0 & 0 & 0 \\ 0 & 0 & \varepsilon_3 & 0 & 0 & 0 \\ 0 & 0 & 0 & \varepsilon_4 & 0 & 0 \\ 0 & 0 & 0 & 0 & \varepsilon_5 & 0 \\ 0 & 0 & 0 & 0 & 0 & \varepsilon_6 \end{pmatrix}. \quad (13)$$

Our results are similar to results found in [8] for $h = 0$.

Calculation of energy eigenvectors in half-filled two-site Hubbard model

First of all, we want to stress that the usage of energy eigenvalue matrix of Eq.(13) is not useful to obtain the eigenvectors. Then, we show an example of how calculating the energy eigenvectors from the basis vectors of Eq.(4),

$$\begin{pmatrix} U & 0 & -t & -t & 0 & 0 \\ 0 & J_1 & 0 & 0 & 0 & 0 \\ -t & 0 & J_2 & 0 & 0 & -t \\ -t & 0 & 0 & J_2 & 0 & -t \\ 0 & 0 & 0 & 0 & J_1 & 0 \\ 0 & 0 & -t & -t & 0 & U \end{pmatrix} \begin{pmatrix} c_1 \\ c_2 \\ c_3 \\ c_4 \\ c_5 \\ c_6 \end{pmatrix} = \varepsilon_n \begin{pmatrix} c_1 \\ c_2 \\ c_3 \\ c_4 \\ c_5 \\ c_6 \end{pmatrix}, \quad (14)$$

the c_i are the components of the eigenvectors. To find out the values of these constants, we have to form the correspondent linear equations. Now, as an illustrative example, we obtain the respective eigenvector for $\varepsilon_2 = U$ forming a system of six algebraic equations given by

$$\begin{aligned} Uc_1 - tc_3 - tc_4 &= Uc_1, \\ J_1c_2 &= Uc_2, \\ Uc_1 - J_2c_3 - tc_6 &= Uc_3, \\ -tc_1 + J_2c_4 - tc_6 &= Uc_4, \\ J_1c_5 &= Uc_5, \\ -tc_3 - tc_4 + Uc_6 &= Uc_6. \end{aligned} \quad (15)$$

In order to solve this system of linear equations, we utilize the normalization condition, *i.e.* the total sum of probabilities is equal to one, $c_1^2 + c_2^2 + c_3^2 + c_4^2 + c_5^2 + c_6^2 = 1$; also we take into account the fact that the eigenvector basis have to be an orthonormal to each one. Therefore, the solutions for Eq.(15) are the following

$$\begin{aligned} c_1 &= \frac{1}{\sqrt{2}}, c_2 = 0, & c_3 &= 0, \\ c_4 &= 0, & c_5 &= 0, & c_6 &= -\frac{1}{\sqrt{2}}. \end{aligned} \quad (16)$$

Then the eigenvector for $\varepsilon_2 = U$ can be expressed as column vector or in the ket notation. We find the 6 eigenvectors given by

$$\begin{aligned}
 X_1 &= \frac{1}{\sqrt{2}} \begin{pmatrix} 0 \\ 0 \\ 1 \\ 1 \\ 0 \\ 0 \end{pmatrix} & X_2 &= \frac{1}{\sqrt{2}} \begin{pmatrix} 1 \\ 0 \\ 0 \\ 0 \\ 0 \\ -1 \end{pmatrix} \\
 X_3 &= a_1 \begin{pmatrix} 1 \\ 0 \\ 0 \\ 0 \\ 1 \end{pmatrix} - a_2 \begin{pmatrix} 0 \\ 0 \\ 1 \\ 0 \\ 1 \end{pmatrix} \\
 X_4 &= a_2 \begin{pmatrix} 1 \\ 0 \\ 0 \\ 0 \\ 1 \end{pmatrix} + a_1 \begin{pmatrix} 0 \\ 0 \\ 1 \\ 1 \\ 0 \end{pmatrix} \\
 X_5 &= \frac{1}{\sqrt{2}} \begin{pmatrix} 0 \\ 1 \\ 0 \\ 0 \\ 0 \\ 0 \end{pmatrix} & X_6 &= \begin{pmatrix} 0 \\ 0 \\ 0 \\ 0 \\ 1 \\ 0 \end{pmatrix}, \quad (17)
 \end{aligned}$$

where a_1 and a_2 are

$$\begin{aligned}
 a_1 &= \frac{1}{2} \sqrt{1 + \frac{U - J_2}{2C}} \quad \text{and} \\
 a_2 &= \frac{1}{2} \sqrt{1 - \frac{U - J_2}{2C}}, \quad (18)
 \end{aligned}$$

respectively.

Furthermore, grouping the eigenvectors in bracket notation, we show that

$$\begin{aligned}
 |\Phi_1\rangle &\equiv \begin{pmatrix} 1 \\ 0 \\ 0 \\ 0 \\ 0 \\ 0 \end{pmatrix}, |\Phi_2\rangle \equiv \begin{pmatrix} 0 \\ 1 \\ 0 \\ 0 \\ 0 \\ 0 \end{pmatrix}, |\Phi_3\rangle \equiv \begin{pmatrix} 0 \\ 0 \\ 1 \\ 0 \\ 0 \\ 0 \end{pmatrix}, \\
 |\Phi_4\rangle &\equiv \begin{pmatrix} 0 \\ 0 \\ 0 \\ 1 \\ 0 \\ 0 \end{pmatrix}, |\Phi_5\rangle \equiv \begin{pmatrix} 0 \\ 0 \\ 0 \\ 0 \\ 1 \\ 0 \end{pmatrix}, |\Phi_6\rangle \equiv \begin{pmatrix} 0 \\ 0 \\ 0 \\ 0 \\ 0 \\ 1 \end{pmatrix}. \quad (19)
 \end{aligned}$$

Therefore, the energy eigenvectors are

$$\begin{aligned}
 |E_1\rangle &= \frac{1}{\sqrt{2}} (|\Phi_3\rangle + |\Phi_4\rangle), |E_2\rangle = \frac{1}{\sqrt{2}} (|\Phi_1\rangle - |\Phi_6\rangle) \\
 |E_3\rangle &= a_1 (|\Phi_1\rangle + |\Phi_6\rangle) - a_2 (|\Phi_3\rangle - |\Phi_4\rangle), \\
 |E_4\rangle &= a_2 (|\Phi_1\rangle + |\Phi_6\rangle) + a_1 (|\Phi_3\rangle + |\Phi_4\rangle), \\
 |E_5\rangle &= |\Phi_2\rangle \quad \text{and} \quad |E_6\rangle = |\Phi_5\rangle. \quad (20)
 \end{aligned}$$

The third version of the Nonextensive Statistical Mechanics

We begin defining the Tsallis entropy [5, 6] as

$$S_q = k_B \frac{1 - \sum_i p_i^q}{q - 1}, \quad (21)$$

where p_i^q is the probability distribution to find the system in i -th state, q indicating the entropic index and k_B is the Boltzmann constant; $\sum_i p_i^q$ symbolizes the quantum operation of trace over all states of the matrix p_i^q . The limit when q tends to 1 of Eq.(21) allow us to recover the well known Boltzmann-Gibbs-Shannon entropy given by

$$S = -k_B \sum_i p_i \ln p_i. \quad (22)$$

The nonextensive probability distribution p_i is obtained through maximum entropy method, which was suggested by the American Edward T. Jaynes [11]. In such procedure, we consider the following constraints

$$\sum_i p_i = 1 \quad \text{and} \quad U_q = \frac{\sum_i p_i^q \varepsilon_i}{\sum_i p_i^q}, \quad (23)$$

where ε_i is the energy eigenvalues. Using the maximum entropy method, we obtain the probability distribution as

$$p_i = \frac{[1 - (1 - q)\beta' \varepsilon_i]^{\frac{1}{1-q}}}{Z_q}, \quad (24)$$

where Z_q is the partition function given by

$$Z_q = \sum_i [1 - (1 - q)\beta' \varepsilon_i]^{\frac{1}{1-q}}, \quad (25)$$

and β' is the energy parameter defined as

$$\beta' = \frac{1}{k_B T}. \quad (26)$$

Evidently, on the limit $q \rightarrow 1$ we recover the standard distribution

$$p_i = \frac{\exp(-\beta \varepsilon_i)}{\sum_i \exp(-\beta \varepsilon_i)}. \quad (27)$$

We want to emphasize in the Eqs.(24) and (25) that is necessary to impose a condition that guarantee the positivity of probabilities. It is named the Tsallis cut-off and defined as

$$1 - (1 - q)\beta' \varepsilon_i \geq 0, \quad (28)$$

so that the probability distribution is

$$p_i = \begin{cases} \frac{[1 - (1 - q)\beta' \varepsilon_i]^{\frac{1}{1-q}}}{Z_q}, & \text{if } 1 - (1 - q)\beta' \varepsilon_i \geq 0, \\ 0, & \text{otherwise.} \end{cases} \quad (29)$$

Furthermore, we can rewrite the relationships for S_q and p_i using the so-called q -exponential function and the q -logarithmic function given by

$$\exp_q(x) = [1 + (1 - q)x]^{\frac{1}{1-q}} \quad \text{and} \quad (30)$$

$$\log_q(x) = \frac{x^{1-q} - 1}{1 - q}; \quad (31)$$

therefore, the formulas for S_q and p_i , Eq.(21) and Eq.(24), are expressed as

$$S_q = -k \sum_i p_i \log_q p_i \quad \text{and} \quad (32)$$

$$p_i = \frac{\exp_q(-\beta' \varepsilon_i)}{\sum_i \exp_q(-\beta' \varepsilon_i)}, \quad (33)$$

respectively, which remember the entropy and probability distribution for the Boltzmann-Gibbs-Shannon's statistics.

For other side, there exists an alternative approach which utilize the following probability distribution

$$p_i = \frac{[1 - (q - 1)\beta' \varepsilon_i]^{\frac{1}{1-q}}}{Z_q}, \quad (34)$$

when q tends to 1, this expression approaches to standard distribution of Eq.(27). And, Z_q is defined by

$$Z_q = \sum_i [1 - (q - 1)\beta' \varepsilon_i]^{\frac{1}{1-q}}. \quad (35)$$

We used these last two equations along with the Eq.(26), what contains the physical temperature T , for our calculations. Notwithstanding, some authors consider other temperature concepts and it continue to be an open problem yet [12,13]. The answer to the question of why we utilize the probability distribution of Eq. (34) is because we find out that, to q varying between 1 and 2, this expression is more appropriate.

Quantum mean values

In the third version of the Nonextensive Statistical Mechanics, thermal mean values of observable O , represented by the operator \hat{O} in the Hilbert space is calculated by

$$O = \langle \hat{O} \rangle = \frac{\sum_i p_i^q O_i}{\sum_i p_i^q}, \quad (36)$$

where O_i standing for the eigenvalues of the observable \hat{O} . The limit when $q \rightarrow 1$ of the last formula become the standard expression

$$O = \langle \hat{O} \rangle = \sum_i p_i O_i. \quad (37)$$

For instance, the internal energy is given by

$$U = \langle \hat{H} \rangle = \frac{\sum_i p_i^q \varepsilon_i}{\sum_i p_i^q}, \quad (38)$$

his derivative with respect to temperature, we get the specific heat

$$C_e = \frac{\partial U}{\partial T}. \quad (39)$$

The magnetization is calculated by

$$M = \langle \hat{\mu} \rangle = \frac{\sum_i p_i^q \mu_i}{\sum_i p_i^q}, \quad (40)$$

where μ_i are the eigenvalues for the quantum operator of magnetic dipolar momentum $\hat{\mu}$.

Results

We employ the programming language Matlab 7.0 for doing computer simulations of the thermodynamic properties such as the entropy per dimer, the internal energy per dimer, the magnetization per dimer and the specific heat per dimer. For the simulations, we assume the relation $J_1 = J_2 \equiv J$ from the contribution of intersite interaction, and $k_B = 1$ for the Boltzmann constant. Moreover, we define the normalized variables $T_t \equiv \frac{T}{t}$, $U_t \equiv \frac{U}{t}$, $J_t \equiv \frac{J}{t}$ and $h_t \equiv \frac{h}{t}$.

Magnetic thermodynamical parameters

The figure 1 shows the entropy, S_q vs the normalized temperature, T_t , for entropic index values $q =$ given by 1.0 (thick lines), 1.4 (dashed lines), 1.7 (dotted lines) and 2.0 (thin lines). In the Fig.1.a, we have $U_t = 5$, $J_t = 0$ and $h_t = 0$ showing at high temperature for $T_t > 0.3$ that when q increases, the saturation entropy

diminishes; in addition, we notice that at for greater q , the entropy curve became flatter. But, at low temperature, $T_t < 0.15$ the opposite case occurs, *i.e.*, for greater q , the greater saturation entropy is observed. Therefore, exist a critical temperature region between $T_t = 0.15$ and $T_t = 0.3$. In Fig.1.b, the parameters are $U_t = 10$, $J_t = 0$ and $h_t = 0$; we observe at low temperatures, $T_t < 0.09$, when q increases, S_q also increases. But when $T_t > 0.17$ we find that q increases, S_q decreases. Therefore, we have found another critical temperature region for T_t between 0.09 and 0.17. In Fig.1.c and Fig.1.d, the parameters U_t and H_t are the same as Fig.1.a and Fig.1.b, respectively. But, considering the interplay between neighbor sites for each dimer,

$J_t = 0.1$ and $J_t = 0.2$ for Fig.1.c and Fig.1.d, respectively. The Fig.1.c shows a crossover temperature region between $T_t = 0.10$ and $T_t = 0.27$. Above this region for high q values, the entropy diminishes; below this region for high q 's, the entropy increases. In Fig.1.d, the increases of J_t shows the absence of the critical region, and a small shifting towards high temperatures is observed. A possible explanation of this effect should be that a little increases in the interactions between neighbours sites of the dimer, J_t , modify the values of all parameters inside the Tsallis cut-off, Eq. (28), so some further zero-probability events happen, and change the quantum mean values.

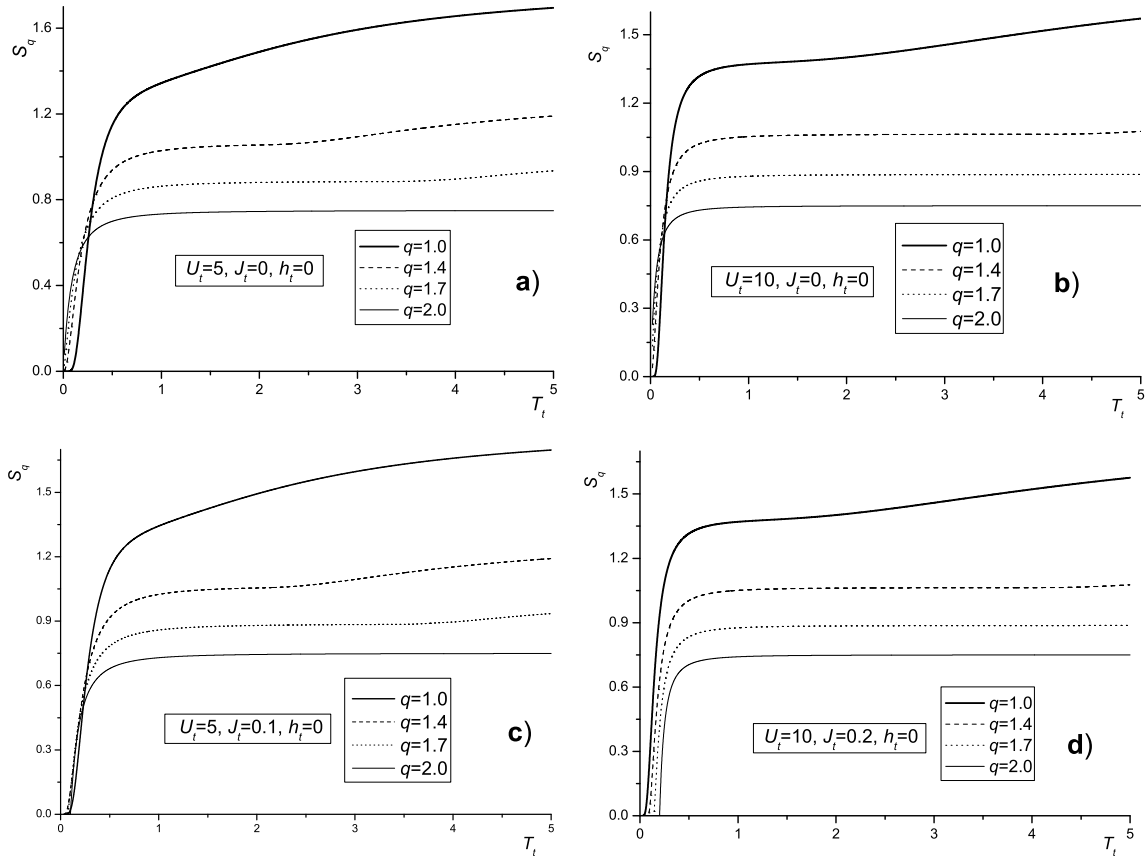


Figure 1: Entropy vs normalized temperature are shown. The values for U_t , J_t and h_t are indicated inside each figure. For $q = 1.0$ (thick lines), $q = 1.4$ (dashed lines), $q = 1.7$ (dotted lines) and $q = 2.0$ (thin lines) the entropy evolution are shown.

The figure 2 show the normalized internal energy E_{int} vs the normalized temperature T_t , for q values given by 1.0 (thick lines), 1.4 (dashed lines), 1.7 (dotted lines) and 2.0 (thin lines). The difference between the Fig.2.a and Fig.2.c (left side), and the Fig.2.b and

Fig.2.d (right side), are that $U_t = 5$ in the first case (left) and $U_t = 10$ in the second (right), and shows that the energy evolution is high for low values of q and U_t and the internal energy saturate quickly for a small increases of q values and high values of U_t . Finally,

for $J_t \neq 0$ the crossover transition observed in Fig.2.a and Fig.2.b (top side) for $J_t = 0$, vanish in Fig.2.c and

Fig.2.d (down side) generating an internal energy saturation for low temperatures.

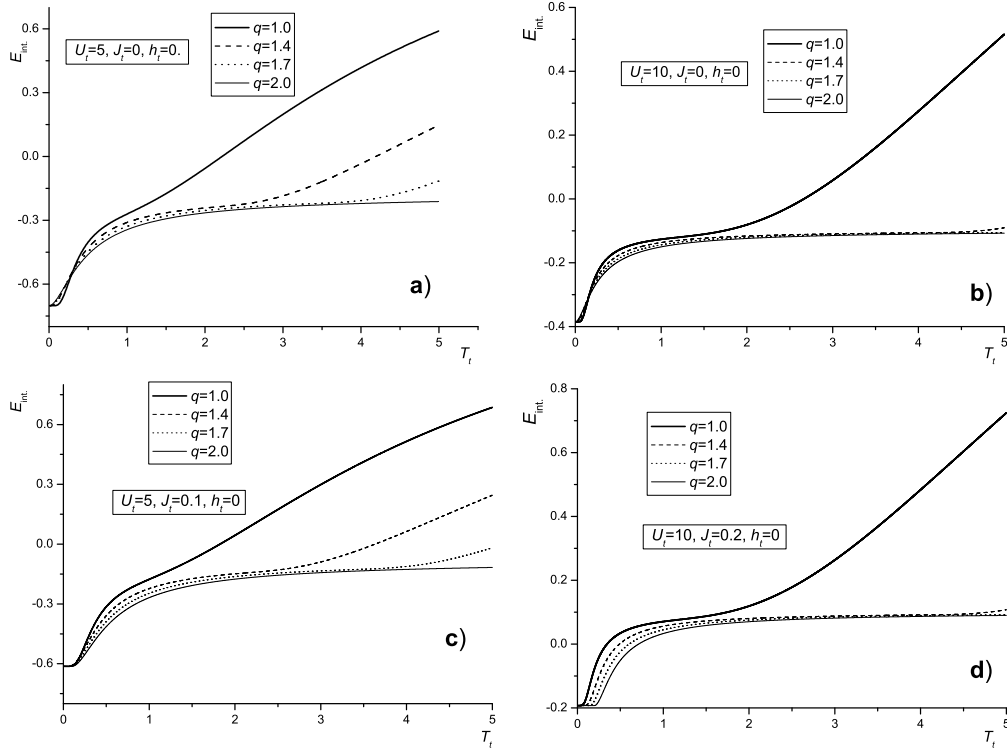


Figure 2: Internal energy *vs* normalized temperature. Inside each figure are indicated the respective values for q , U_t , J_t and h_t . In a) and b), we have no interaction between neighbor sites for each dimer. But, in c) and d), we consider a non-zero intersite interaction.

When a magnetic field is applied to the system the response is show in figure 3, where the magnetization M *vs* normalized temperature, T_t , are displayed with the entropic index $q =$ given by 1.0 (thick lines), 1.4 (dashed lines), 1.7 (dotted lines) and 2.0 (thin lines). In Fig.3.a, we have calculated M using $U_t = 5$, $J_t = 0$ and $h_t = 8$ and the results show a critical temperature region for T_t near to 4.5 and 5.7. Above this region the magnetization get smaller for low q values meanwhile below this region the magnetization became greater for low q values to finish in saturation at low temperatures. Comparing with Fig.3.b, where $U_t = 10$ the behaviour of the magnetization are similar, but with the critical temperature shifting near to 5.0 and 5.7. In the Fig.3.c and Fig.3.d, the $J_t = 0.1$ and $J_t = 0.2$, respectively. In both cases the behaviour of the magnetization are similar to the a) and b). For the left case, a) and c) the saturation occurs at low temperatures meanwhile for he right case, b) and d) the saturation have a small shift to the right.

The figure 4 show the specific heat at constant volume, C_V , *vs* the normalized temperature, T_t , with entropic index $q =$ values such as 1.0 (thick lines), 1.4 (dashed lines), 1.7 (dotted lines) and 2.0 (thin lines). In the Fig.4.a, we use $U_t = 5$, $J_t = 0$ and $h_t = 0$; in the Fig.4.b, we set up $U_t = 10$, $J_t = 0$ and $h_t = 0$. In the Fig.4.c and Fig.4.d, the parameters are the same except that intersite interaction $J_t = 0.1$ and $J_t = 0.2$, respectively. In these figures, excepting the curve with $q = 2.0$, in the left side (a and c), which has only one peak, we observe two peaks for all values of q , the first peak is due to antiparallel order at low temperatures meanwhile the second more broadened is provoked by metal-insulator transition at high temperatures. For other side, certainly the effect on the specific heat curves are strong with high value of U_t at high temperatures and the broadened remains only for low values of q in the right side (c and d). The effect of high values of J_t is shifting the specific heat curves for high temperatures values.

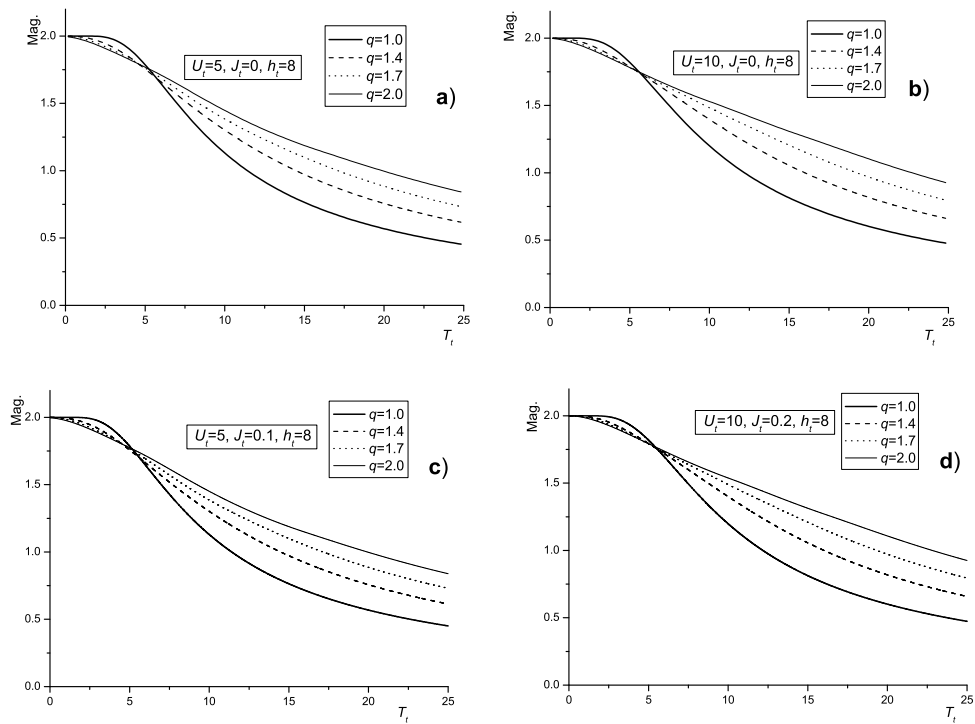


Figure 3: Magnetization *vs* normalized temperature. The values for q , U_t , J_t and h_t are given in the figures. In a y b, there is not intersite interaction, meanwhile in c and d, these are 0.1 and 0.2, respectively.

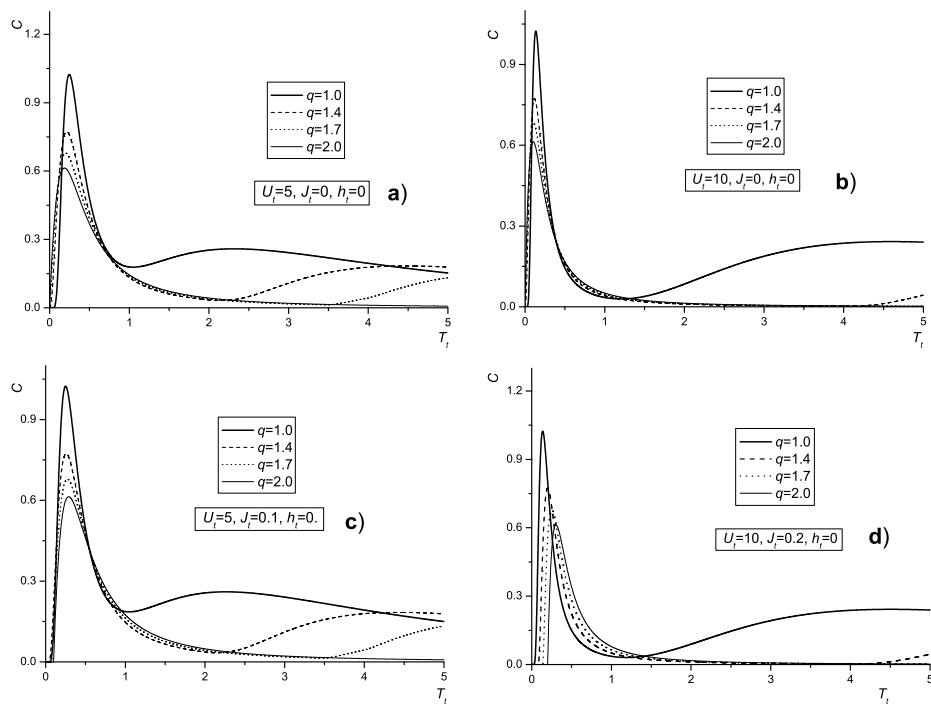


Figure 4: Specific heat *vs* normalized temperature. The values for q , U_t , J_t and h_t are given inside each figure. For a and b, we have not intersite interplay. But, in c and d we consider $J_t = 0.1$ and $J_t = 0.2$, respectively.

Conclusions

We have analyzed M dimers with a half-filled two-site Hubbard model using the third version of nonextensive statistical mechanics as tool for calculating normalized entropy, internal energy and specific heat. This statistical theory would be the correct for researching small systems, in this case a one-dimensional system. The computer simulations for Hubbard model with only the on-site term are in total agreement with previous results. The addition of intersite interaction term produces a shift in all the parameter curves. This would be

due to the intersite interaction term what modifies the parameters inside the Tsallis cut-off. We conclude that the probability distribution used with the q values between 1 and 2 are adequate for researching the extended Hubbard model.

Acknowledgements

We are extremely grateful to Professor M. Matlak, University of Silesia, Poland, for give us notice about important references for our research.

Referencias

- [1] H. Hasegawa, Physica A **351**, 273 (2005). H. Hasegawa, Physica A **390**, 1486 (2011). arXiv:cond-mat/0410045v5 (2005).
- [2] J. Hubbard, *Electron Correlations in Narrow Energy Bands*, Proc. Roy. Soc. of London. A, Math. & Phys. Sci., **276**(1365), 238 (1963).
- [3] H. Tasaki, J. Phys.: Condens. Matter **10**, 4353 (1998).
- [4] Fabian H. L. Essler, Holger Frahm, Frank Göhmann, Andreas Klümper and Vladimir E. Korepin; *The One-Dimensional Hubbard Model*, Cambridge (2005).
- [5] Constantino Tsallis and Ugur Tirnakli, J. Phys.: Conf. Series **201**, 012001 (2010).
- [6] C. Tsallis, Phys D **193**, 3 (2004). G. L. Ferri, S. Martinez and A. Plastino, J. Stat. Mech. P04009 (2005). arXiv:cond-mat/0503441. <http://tsallis.cat.cbpf.br/biblio.htm>.
- [7] C. Tsallis, R.S. Mendes and R. Plastino, Physica A **261**, 534 (1998).
- [8] M. Matlak, B. Grabiec, S. Krawiec, J. Non-Cryst. Sol. **354**, 4326 (2008). arXiv:cond-mat/0511329v1 (2005).
- [9] Marcelo A. Macedo and Claudio A. Macedo, *Thermodynamics of the Two-Atom Hubbard Model*; Rev. Bras. Ens. Fis. **21**(3), 321 (1999).
- [10] C. Tsallis, J. of Stat. Phys **52**, 479. (1988).
- [11] E. T. Jaynes, *Information Theory and Statistical Mechanics*, Phys. Rev. **106**, 620 (1957). E.T. Jaynes. *Lectures in Theoretical Physics 3: Statistical Physics*, p.181, Ed. K.W. Ford, Bryeis University (1963).
- [12] S. Abe, S. Martinez, F. Pennini and A. Plastino, Phys. Lett. A **281**, 126 (2001).
- [13] C. Tsallis, *Introduction to Nonextensive Statistical Mechanics: Approaching a Complex World*, Springer, New York, (2009).